Modeling and Analysis of Aberrations in Electron Beam Melting (EBM) Systems

Armin Azhirnian[1], David Svensson[2]
[1]Chalmers University of Technology, Gothenburg, Sweden
[2]Arcam AB, Mölndal, Sweden

***Abstract*—Arcam AB has pioneered additive manufacturing with the electron beam melting (EBM) technology that is used for a cost efficient and novel ways of producing components in titanium for the orthopaedic and the aerospace industries. The electron beam is at the heart of the EBM technology, where beam-quality is directly related to the performance of the EBM machine. The beam is controlled with magnetic lenses, which are known to cause aberrations. We present a modeling framework which can be used to study aberrations, as described in the literature for electron microscopy, in an electron beam melting (EBM) system. This is achieved by using the COMSOL Multiphysics® simulation software to solve for the magnetic fields and relativistic charged particle trajectories with space charge of a model EBM system in 3D. This involves formulating a model for the magnetic lenses which performs the functions of focusing, deflecting and correcting the electron beam using magnetic stigmator lenses. For this purpose the combined capabilities of the AC/DC, Particle Tracing and LiveLink™ for MATLAB® modules were used running on a COMSOL Server™.**

I. Introduction

The Arcam electron beam melting (EBM) system uses a series of magnetic coil lenses to focus, deflect and correct an electron beam which melts metal powder in a precisely controlled pattern. A solid understanding of how perturbations and non-ideal conditions effect a system's reliability and performance is essential. This is particularly true when the system process involves non-linear interactions between the different parts of the system. This paper describes how the COMSOL Multiphysics® software [1] can be used to model the aberrations in an EBM system. There is also a description of how the aberrations can be quantified and analyzed with the purpose of mitigating the effect of the aberrations.

A. Electron Optics

The electron beam is focused, steered and corrected using a series of electromagnetic coils. These coils are somewhat analogous to optical elements that focus, steer and correct a ray of light. A system that controls an electron beam in this way is often referred to as an electron optical system. The most important mechanism in any electron optical system is the Lorentz force which is the force acting on a charged particle moving in an electromagnetic field. The force acting on such a charged particle is given by

$$\mathbf{F} = q(\mathbf{v} \times \mathbf{B} + \mathbf{E}). \tag{1}$$

The electron optical system consists of one or a series of electromagnetic fields which perform an optical function such as focusing, deflection or correction. The force is proportional to the cross-product of the velocity of the electron and the magnetic field which means that a magnetic field can not perform any work on the electron. The EBM system that is being modeled used an electrostatic field for the extraction and acceleration of the electron beam and magnetic fields for focusing, deflecting and correction.

1) Focusing Solenoid: The magnetic field from a solenoid with its magnetic axis aligned with the optical axis will focus an electron beam due to the Lorentz force [2]. The focusing coil will also have the secondary effect of rotating the beam in a helical trajectory along the optical axis. It can be shown that a simple focusing coil like this will introduce spherical and chromatic aberrations [3]. The focusing power of a solenoid is given by [4]

$$1/f = \frac{\pi}{16}\frac{e^2}{mE_0}aB_0^2 \tag{2}$$

where E_0 is the acceleration potential of the electrons and B_0 is the magnetic field strength in the solenoid. This mean that for $f = 1\,\mathrm{m}$ and a coil height $a = 10\,\mathrm{cm}$ a field strength $B_0 = 4\,\mu\mathrm{T}$ is required.

2) Deflection Dipole Pair: A deflection coils operates by inducing a magnetic field perpendicular to the optical axis. This results in a Lorentz force that is perpendicular to both the magnetic field and the velocity of the electron as illustrated in figure (1:a). The figure shows how a quadrupole can be used to induce the magnetic field required in a deflection coil. The two dipole pairs are used to induce a deflecting magnetic field with an arbitrary rotation in relation to the optical axis.

If the deflection field is completely homogeneous and the incoming electrons travel along the optical axis, the deflection will eventually make the electrons move in a circle with radius [5]

$$r = \frac{mv_0}{eB_0}. \tag{3}$$

This can be seen from solving the classical equations of motion for an electron in a homogeneous magnetic field $\mathbf{B} = B_0\hat{x}$

$$m\dot{v}_y(t) = \quad B_0 q v_z(t) \tag{4}$$
$$m\dot{v}_z(t) = -B_0 q v_y(t) \tag{5}$$

Differentiating once with respect to time and substituting the velocities we obtain a homogeneous Helmholtz equation. With

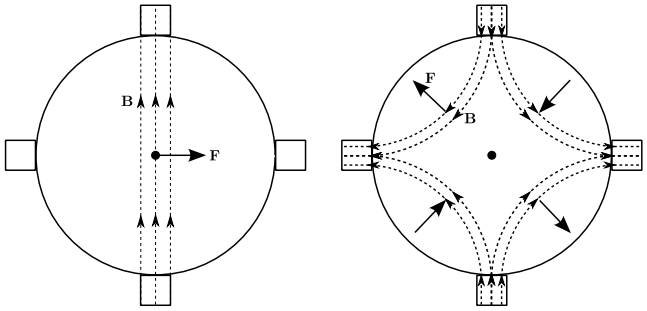

(a) (b)

Fig. 1: Cross section of **(a)** a deflection dipole and **(b)** a quadrupole stigmator showing the magnetic field and resulting forces on an electron moving out of the plane. The magnetic fields are shown as dashed lines and the forces as solid arrows.

the initial conditions

$$v_y(0) = 0 \tag{6}$$
$$\dot{v}_y(0) = \frac{B_0 q}{m} v_0 \tag{7}$$
$$v_z(0) = v_0 \tag{8}$$
$$\dot{v}_z(0) = 0 \tag{9}$$

we obtain the solution

$$v_y(t) = v_0 \sin\left(\frac{qB_0}{m}t\right) \tag{10}$$
$$v_z(t) = v_0 \cos\left(\frac{qB_0}{m}t\right). \tag{11}$$

The deflection angle is then simply

$$\alpha = \arctan\frac{v_y}{v_z} = \frac{qB_0}{m}t. \tag{12}$$

Now assuming that the field is zero for $z > a$ such that $B_0 q/m \gg t_a$ we may substitute $t = z/v_0$ to approximate the angle with

$$\alpha = \frac{B_0 q}{m}\frac{a}{v_0}. \tag{13}$$

As an example a $60\,\mathrm{keV}$ electron in a field that is $10\,\mathrm{cm}$ long and $1\,\mathrm{mT}$ strong will be deflected $120\,\mathrm{mrad}$.

3) Quadrupole Stigmator: A stigmator coil is a quadrupole where the direction of the magnetic field alternates as shown in figure (1:b). The resulting force field will deform the electron beam in the shape of an ellipse. This is used to correct the beam astigmatism induced by the electron optical system and the geometry of a deflected beam. The quadrupole stigmator can only correct aberration with a two-fold symmetry. Higher order stigmators can both be used alone or in series to correct higher order aberrations [6].

4) Aberrations: In order to know the performance of the aberration correction, we need a formalism for describing the aberrations.

Gaussian optics describes the concept of perfect focusing lenses that maps plane waves propagating along an optical axis $\hat{z}$ to spherical waves converging at some focal point on that same axis. This ideal lens is used as a reference and the distance of the resulting wave front from the ideal wave front is defined as the error. Typically the error W is a scalar field in two dimensions that is converted to phase representation called the wave aberration function $\chi = (2\pi/\lambda)\, W$.

TABLE I: Complex Wave Aberration basis functions with names from [8]. The first 7 functions are written here. Note that the basis is not normalized here.

Index	Name	Power	Symmetry	Expression
1	Shift	1	1	$\bar{\omega}$
2	Defocus	2	0	$\omega\bar{\omega}$
3	Twofold astigmatism	2	2	$\bar{\omega}^2$
4	Second-order axial coma	3	1	$\omega^2\bar{\omega}$
5	Threefold astigmatism	3	3	$\bar{\omega}^3$
6	Third-order spherical aberration	4	0	$\omega\bar{\omega}^2$
7	Third-order star-aberration	4	2	$\omega^3\bar{\omega}$

Moving on, we would also be interested in the resulting image in the Gaussian focal plane given a wave aberration function χ. We define the image aberration δ as the two dimensional vector field in the Gaussian plane measuring the displacements of our aberrated beams from the ideal beam. The relation between wave and image aberrations is

$$\delta(x,y) = \frac{M\lambda}{\pi}\nabla\chi(x,y) \tag{14}$$

with M the magnification of the optical system. Using the above relation we can avoid the problem of measuring phase, instead comparing images to quantify aberrations.

A common way to express the wave aberration function in electron optics is

$$\chi(\theta,\phi) = \frac{\theta^{N+1}}{N+1}\big(C_{NSa}\cos(S\phi) + C_{NSb}\sin(S\phi)\big) \tag{15}$$

with θ inclination and ϕ azimuth in spherical coordinates [7].

In practice the wave aberration function can be hard to find and manufacturers of adaptive electron optics have chosen to measure the image aberration $\delta(x,y)$ instead. Now let

$$\omega = x + iy \tag{16}$$

represent our position vectors with $\bar{\cdot}$ denoting complex conjugation. Then we have the complex wave aberration function

$$W(\omega,\bar{\omega}) = \Re\sum_{N,M} c_{N,M}\omega^N\bar{\omega}^M. \tag{17}$$

Using some of the multiplication properties of complex numbers we note that the power is $p = N + M$ and the symmetry $s = |N - M|$. We further add implicit rules for N and M to get uniqueness for our representation. This is done by requiring $p \geq s$ and that p and s share the same parity. With these rules we find ourselves with the basis described in table I.

The gradient in Euclidean space is equivalent to

$$2\frac{\partial W}{\partial\bar{\omega}} \tag{18}$$

in the complex plane [8]. Using this formulation the gradient lies in the complex plane as well, making calculations such as least squares fitting rather convenient.

B. Electromagnetic Fields

We have seen that through the Lorentz Force, electrons are affected by both electric and magnetic fields. In EBM, Electric fields emerge from the voltage between the cathode and the ground plane as well as from the negatively charged electrons themselves. The electron optics is the largest source of magnetic fields while the magnetic fields of the moving electrons has a negligible effect on their trajectories. Limiting the scope of this paper to optics that generate only static magnetic fields, we may use the following of Maxwell's equations:

$$\nabla \times \mathbf{H} = \mathbf{J} \tag{19}$$

$$\nabla \cdot \mathbf{B} = 0. \tag{20}$$

Treating the electrons as point particles, the electric field emerging from them is

$$\mathbf{E}(\mathbf{r}) = \sum_{i}^{N} \frac{q}{4\pi\epsilon_0} \frac{\mathbf{r} - \mathbf{r_i}}{|\mathbf{r} - \mathbf{r_i}|^3} \tag{21}$$

where $\mathbf{r}_i$ denotes the time dependent position of the electron i. Clearly enumerating every electron of a beam in a volume on the order of cubic centimeters is not a viable approach for computation. A more suitable method is to reduce the positions and combined charges of electrons to a space charge density, and use that for calculating electric fields.

II. Method

Both the magnetic fields and the trajectories of the electrons need to be solved for when analyzing the aberrations of an electron optical system. COMSOL Multiphysics® with the AC/DC module solves the magnetic fields using a Finite Element Method. The solution can then be used with the COMSOL Particle Tracing Module to find the trajectories of the electrons that pass through the lenses.

The models are solved in two separate solver steps. The first step contains a stationary solver which solves the static magnetic fields from the magnetic coils. This solution is used as an input to the second step which is an iterative Bidirectionally Coupled Particle Tracing study. This ensures that the solver reaches a self-consistent solution in regards to the particle trajectories and the beam space-charge.

Throughout the simulation, gigabytes of data are generated. For managing and post processing the data, controlling the simulations and making advanced parametrization studies possible, the scripting capabilities included in LiveLink for MATLAB are used.

A. Modeling multipoles in COMSOL Multiphysics®

One of the problems in modeling an electron optical system is formulating an accurate description of the coils that constitute the magnetic lenses. On one hand, there is a need to include as much detail as possible in the coil-models in order to capture the effects of geometrical asymmetries and perturbations on the electrons' trajectories. On the other hand, the finite element method used to compute the magnetic fields and electron trajectories imposes limits on the geometric complexity of the models. These limits result from the fact that the number of elements, and therefore number of degrees of freedom, increase with the geometric complexity which in turn increase both the memory requirement and the time needed to solve the model.

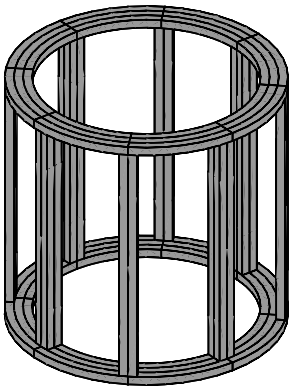

Fig. 2: Geometric model of a quadrupole coil. Each pole consists of 3 coils that have an angular width of $\pi/4$ meaning that the coil is split into 3 shells with different radii.

Separate considerations also need to be taken in relation to how the currents in the coils are modeled. In an ideal model each wire in the coil would be modeled separately, both in terms of geometry and current. This is not feasible when the scale of a single wire is significantly smaller than the surrounding geometry. COMSOL Multiphysics® circumvents this by modeling the wires in a multi-turn coil by defining a vector-field describing the current directions in a geometric domain. The deflection and astigmatism coils used in Arcam's EBM machines consist of 4 air-wound coil with a sinusoidal turn distribution. This means that each coil must be modeled using several COMSOL coils in order to describe the actual wire distribution.

One simple way to model a quadrupole coil is to simplify the sinusoidal distribution to only 3 circular coils place along a cylinder as shown in figure 2. This type of coil model has a simple geometry consisting of vertical bars and horizontal circular segments. Each pole is composed of 3 coils that each have an angular width of $\pi/2$. This means that the quadrupole needs to consist of 3 separate layers(or shells) in order to fit a quadrupole.

The technique used to generate the coil geometry shown in figure 2 becomes very complicated if it is used to generate coils with 12, 24 or 48 poles. This led to the development of a new way to generate the geometry and define the coil properties for coils with an arbitrary pole configuration.

We call this coil modeling technique "the superposition model" since it is based on the assumption that 2 neighboring coil segments with the same current direction can be superimposed into one geometry. This assumption is valid if the

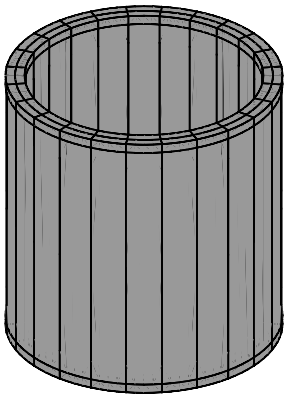

Fig. 3: Geometric model of a multipole coil. The segments in the model can be used to implement coils with arbitrary pole configurations.

distance between the coil segments is much shorter than the distance to the beam, i.e. the center of the coil. The geometric model used for the superposition coils is shown in figure 3.

The modeling works by assigning a pre-calculated current to each geometric domain the the model using a MATLAB script. While it would be possible to define the coil properties manually in the COMSOL Multiphysics® GUI, it would be both time consuming and error prone.

One advantage of the superposition model is that it is possible to model a coil with many different multipole, each with different currents, within the same geometry. This allows the user to try different coil-, pole- or current-configurations by only altering the individual currents accordingly.

B. Meshing the model

It would be possible to use the automatic meshing function in COMSOL Multiphysics® without any tuning and get satisfactory results. However, in case of modeling charged particle tracing and magnetostatic fields at the same time there is room for manual improvement. This is due to the large difference in scale between the magnetic lenses and the size of the electron beam. This problem is even more prominent since the models includes a space charge effect between the electrons. The meshing process is therefore modified such that the size of the mesh elements is much smaller in the regions where the electron beam is expected to be, as shown in figure 4. This will minimize the error in the beam trajectory modeling without needlessly increasing the number of mesh elements in volumes only occupied by the magnetic fields.

C. Quantifying the aberrations

Finding the aberrated equivalent to a focal point was done in the post processing step in MATLAB. The particle phase space data was given by COMSOL Multiphysics® at the time steps solved for. In MATLAB linear interpolation was

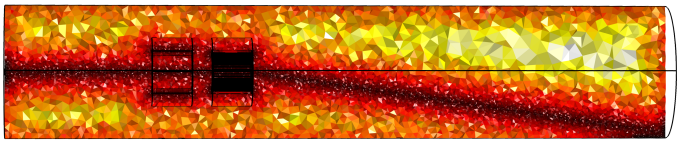

Fig. 4: Cut through of the mesh used in the COMSOL model where the color corresponds to the size of the mesh elements. Note how the fine mesh structure follows the expected beam path after the deflection coil.

used to trace the particles between the time steps of the solution. Further on a routine for making Poincaré sections was made so that the images at different distances along the optical axis could be viewed. On these sections we could then evaluate measures of confusion and then run one of MATLAB's optimization tools to find the plane of least of least confusion.

First we simulated a reference beam, that was only focused without any deflection or aberration correction. This beam took the place of the Gaussian beam in optics and all aberrations were measured using it as a reference.

These samples were then fit to the gradient of the truncated series of the Wave Aberration Function with MATLAB's backslash routine. Since the coefficients in the gradient are the very coefficients of the Wave Aberration Function the aberration spectrum was then extracted.

III. Results

Both fields and trajectories were studied. The fields of interest were those of thick magnetic multipoles that were generated using our parametrization. In particular the field around the z axis must be investigated in order to be certain that spurious solutions have not been found. For the trajectories, problems with known solutions were chosen so that they may serve as a verification of the model. Focal distance and deflection angles are examples of such.

One of the major advantages of the superposition coil model is the fact that many different order stigmator coils can be modeled without altering the geometry of the coil. This is shown in figure 5 where the magnetic field from stigmators with the symmetry order 4, 6, 8, 12, 16 and 24 are plotted.

In figure 7 the relation between current times number of turns and deflected distances at the wall is shown for an setup with deflection and focus only. The beam entered the model at the origin and traversed the focus lens at $220\,\mathrm{mm}$ and the deflection lens at $310\,\mathrm{mm}$ until finally hitting the wall at $1000\,\mathrm{mm}$.

In one experiment the deflection field originated from only one dipole aligned at a right angle to the desired deflection with current I. In the other experiment the field was solved for two orthogonal dipoles at $45°$ from the direction of the desired deflection with currents I_x and I_y respectively. In the case with two dipoles the currents were normalized as $\sqrt{I_x^2 + I_y^2} = I$ and the number of turns per coil the same as in the single dipole model. The magnetic fields along the z-axis are presented in figure 6 for a single setting for the single dipole.

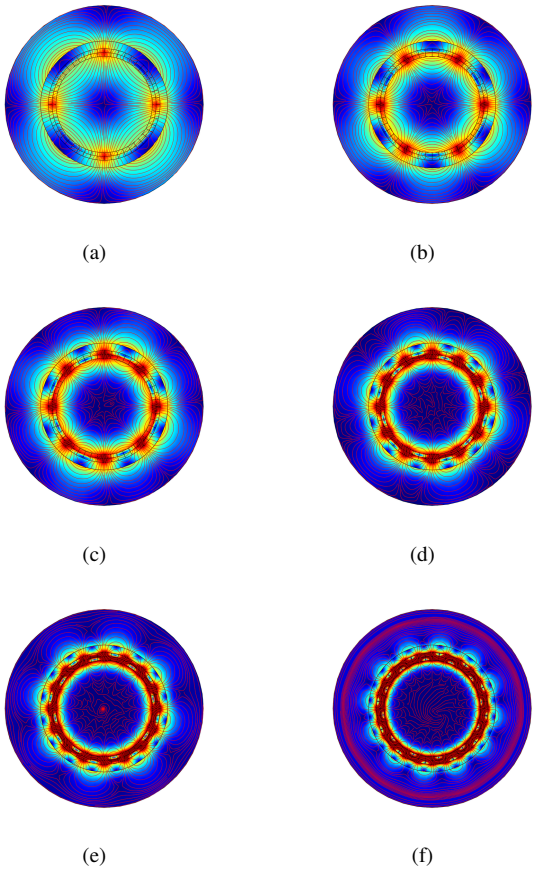

Fig. 5: Plots of magnetic fields resulting from stigmators with symmetry order 4, 6, 8, 12, 16 and 24. The field direction are plotted as red streamlines and the field magnitude is shown as the colored background where red corresponds to the largest magnitude. Note that the magnitude approaches zero at the center of the lens which results in an unstable estimate of the direction of the magnetic field. This effect is particular noticeable in the stigmators with a higher order of symmetry.

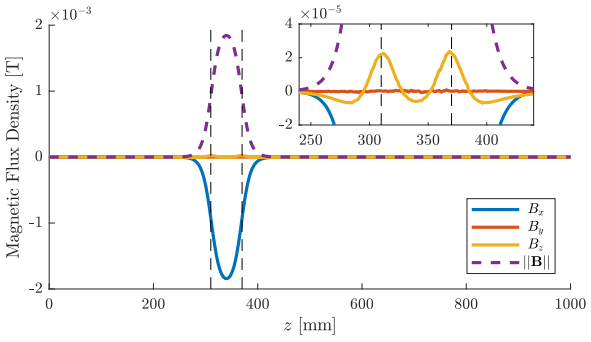

Fig. 6: Magnetic fields on the z-axis from a single dipole deflection lens. The lens physically extends from the left dashed vertical line to the right.

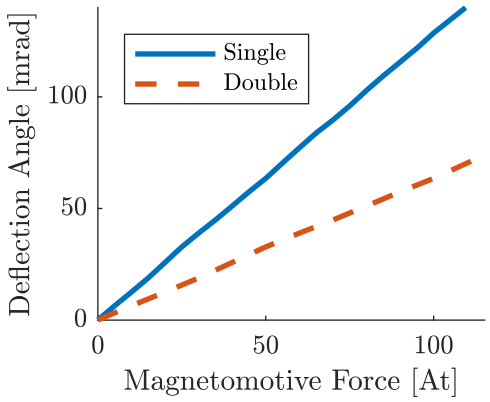

Fig. 7: Deflection angles depending on current and number of turns for a single dipole and a double dipole. The slopes of the single and double dipole curves are $1.2\,\mathrm{mrad/At}$ and $0.6\,\mathrm{mrad/At}$ respectively.

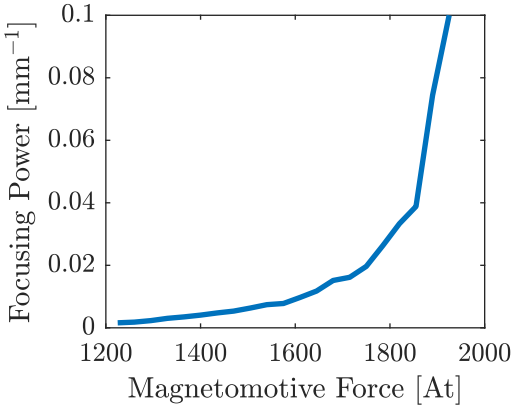

Fig. 8: Focusing power $1/f$ for 24 different settings of the current and number of turns in the focus lens. Focal distance f is measured in mm from the center of the focus lens. The beam size used for finding focus was calculated as the standard deviation of the particles in a cut plane.

A study was made varying the current to the focal lens in a fully deflected system with space charge. The theory presented earlier states that the focusing power should be linear in B_0 for a thins lens neglecting the effect of space charge. In figure 8 the effect of space charge as well as size of the lens can be investigated by observing how the behaviour of the beam changes close as it is focused closer to the lens. Another revelation is how the beam size converges for higher magnetomotive forces.

Studies were made investigating which aberrations are dominant in EBM. In figure 9 a Poincaré section of a beam is shown at its disc of least confusion along with a beam that has been defocused by $15\,\mathrm{mm}$. The densities are shown as the brightness of the color of each electron. One may observe dense rings in the defocused beam and looking at its aberration spectrum in figure 10 defocus and higher order spherical aberration is dominant.

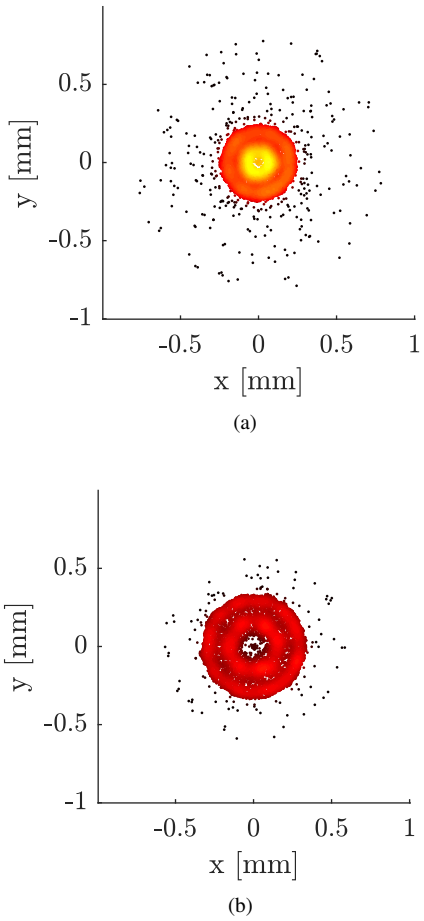

Fig. 9: Cross section of focused beam of 5000 electrons **(a)** along with beam that has been defocused by 15 mm **(b)**. The density is plotted as the brightness of the colors.

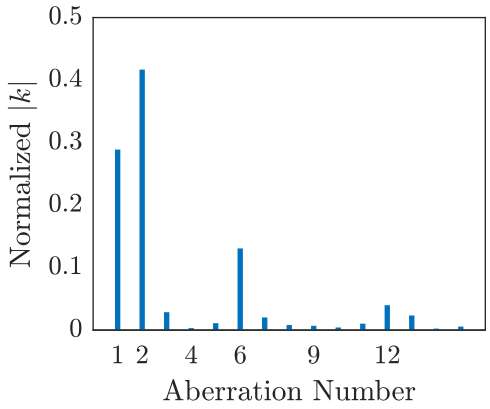

Fig. 10: Spectrum of aberrations for the beam in figure 9. The aberration basis is defined in table I.

IV. Conclusion

We have shown how aberrations in an EBM system can be studied and analyzed using COMSOL Multiphysics®. We have also shown how this model can be used to perform case studies of an EBM system. However, the time constraints imposed by this project has left many of the possible applications of the modeling framework for future studies. There has also been a significant effort to understand the modeling errors and thereby increase the confidence in the results.

Our model has laid a foundation for modeling and understating aberrations in EBM system. However, there are many problems that needs to be solved before the insights gained by our model can be implemented in a physical EBM machine. It has become clear throughout our project that it would be very challenging to mitigate the aberrations without having access to measurements of the actual beam profile in the EBM system. This type of measurements would not only provide a way to verify and improve the models but also function in a feedback based corrections system.

References

[1] COMSOL AB, "Comsol multiphysics®," version 5.3. [Online]. Available: https://comsol.com

[2] H. Rose, *Geometrical Charged-Particle Optics*, 2nd ed. Springer Berlin Heidelberg, 2012, vol. 142.

[3] O. Scherzer, "Über einige fehler von elektronenlinsen," *Zeitschrift für Physik*, vol. 101, no. 9, pp. 593–603, 1936.

[4] R. F. Egerton, *Physical Principles of Electron Microscopy: An Introduction to TEM, SEM, and AEM*, 2nd ed. Cham: Springer International Publishing, 2016.

[5] D. C. Joy, A. D. Romig, and J. I. Goldstein, *Principles of Analytical Electron Microscopy*. Boston, MA: Springer US, 1986.

[6] M. Haider, H. Rose, S. Uhlemann, B. Kabius, and K. Urban, "Towards 0.1 nm resolution with the first spherically corrected transmission electron microscope," *Journal of Electron Microscopy*, vol. 47, no. 5, p. 395, 1998.

[7] R. Brydson, *Aberration-Corrected Analytical Transmission Electron Microscopy*, ser. RMS - Royal Microscopical Society. Wiley, 2011.

[8] R. Erni, *Aberration-corrected imaging in transmission electron microscopy: An introduction*. World Scientific Publishing Co Inc, 2015.